The application of stereolithography to the fabrication of accurate molecular models

William J. Skawinski,* Thomas J. Busanic,* Ana D. Ofsievich,*
Thomas J. Venanzi,† Victor B. Luzhkov,*‡ and Carol A. Venanzi*

*Department of Chemical Engineering, Chemistry, and Environmental Science, New Jersey Institute of Technology, Newark, New Jersey
†Department of Chemistry, College of New Rochelle, New Rochelle, New York
‡Present address: Institute of Chemical Physics, Chernogolovka, Moscow Region, Russia

The process of stereolithography, which automatically fabricates plastic models from designs created in certain computer-aided design programs, has been applied to the production of accurate plastic molecular models. Atomic coordinates obtained from quantum mechanical calculations and from neutron diffraction data were used to locate spheres in the I-DEAS CAD program with radii proportional to the appropriate van der Waals radii. The sterolithography apparatus was used to build the models using a photosensitive liquid resin, resulting in hard plastic models that accurately represent the computed or experimental input structures. Three examples are given to illustrate how the models can be used to interpret experimental structure–activity data for systems of biological importance or host–guest chemistry: (1) Interpretation of kinetic data for the formation of a stable blocking complex between amiloride analogs and the epithelial sodium channel, (2) interpretation of binding and neural activity data for the interaction of certain amino acids and their analogs at the L-alanine taste receptor of the channel catfish, and (3) interpretation of shape selectivity and rate acceleration in cyclodextrin catalysis using models of the neutron diffraction structure of β-cyclodextrin and of the transition state for the cleavage of phenyl acetate by the secondary hydroxyl oxygen of β-cyclodextrin.

Keywords: stereolithography, computer-aided molecular design, plastic models, amiloride, sodium transport, β-cyclodextrin, enzyme mimics, catfish taste.

INTRODUCTION

A number of systems have been developed for fast free-form manufacturing (FFM) or rapid prototyping. The original purpose of these systems was to fabricate models of designs created within a computer-aided design (CAD) program so that they could be used as prototypes in a wide variety of applications. This allows an engineer or designer to make use of all the power of CAD software to create an image and have the FFM system automatically build an accurate three-dimensional model of that image. Here we describe the application of one such system, laser stereolithography, to the automatic fabrication of accurate molecular models and demonstrate their use in investigating experimental structure–activity relationships for molecules of biological and chemical importance.

Stereolithography[1-7] utilizes a computer-controlled helium–cadmium ultraviolet laser to cure a photosensitive liquid resin to yield a solid plastic model. The stereolithography process is described in detail in Methods (below). The data from a CAD program describing an image are used to direct the model-building process.

Many molecular graphics programs produce excellent images of molecular structures. However, to obtain the full three-dimensional effect from a two-dimensional graphics screen, it is necessary to rotate the molecule continually on the screen or to produce stereo pairs of the structures and use special viewing glasses. Often it is useful to have a physical model of these images, but it can be difficult to translate information from the computer display into physical objects. Commercially available products, for example, CPK or Dreiding models, used to make such models are necessarily limited to a relatively small number of atomic shapes and bonding schemes relying on average dimensions and standard components. These models do not necessarily represent torsional relationships accurately and cannot be used to represent molecular properties such as the molecular

electrostatic potential or the dipole moment. An alternative to these commercially available models would be to have each model built individually by highly skilled craftsmen—a process that can be prohibitively expensive and time consuming.

The original impetus for our interest in producing physical models was to assist one of us (W.J.S.), a blind chemist, to perceive molecular structures obtained by *ab initio* molecular orbital conformational analysis. These techniques would then be extended to model other physical phenomena useful to blind and visually impaired researchers in other disciplines. This aspect of our work has been described in detail elsewhere.[8] However, it became apparent that such models could also provide sighted researchers with useful tools for interpreting structure–activity data for applications in such areas as drug design. Models prepared to highlight specific physical features could be used in illustrating aspects of an interpretation, thereby enhancing scientific communication.

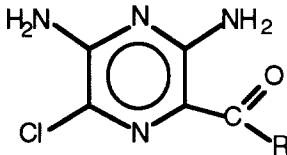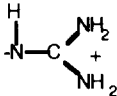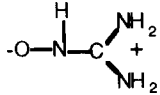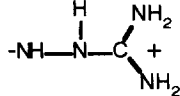## Structure–activity relationships of amiloride analogs

Our first application of this technique to a structure–activity problem was in assisting in the interpretation of the relative efficacy of the diuretic drug amiloride, 1, and its structural analogs 18 and 19[9] as epithelial sodium channel blockers. The two analogs differ from amiloride by the insertion of an –O– or –NH– group, respectively, between the carbonyl carbon and the guanidinium group. Although these modifications increase the length of the side chain and change its geometry, it can be seen from Table 1 that both analogs

retain the ability to bind to and block the sodium channel. In fact, analog 19 is a slightly better blocker than amiloride, as indicated by the reciprocal of k_{off}, which gives the block time or residence time of the molecule at the channel binding site.

From the results of their studies of amiloride analogs with both pyrazine ring and side chain modifications, Li et al.[9,10] have postulated a two-step blocking mechanism governed by two rate constants, k_{on} and k_{off}. The first step involves the positively charged guanidinium side chain interacting with the channel to form an encounter complex. This is then followed by the interaction of the substituent at the 6-position of the pyrazine ring with another site on the channel to form the blocking complex. Substitution at the 6-position by other halogens or hydrogen showed that the most stable complex is formed when the ligand is a chlorine atom (see Table 1).

Because the molecular structure of the ion channel is not known, Venanzi and co-workers have attempted to interpret these structure–activity data at the molecular level by conformational analysis,[11,12] molecular electostatic potential analysis,[13,14] and molecular dynamics and static solvation studies[12,15] of amiloride and its analogs. Much of this work has been summarized in a review article.[16] On the basis of molecular electrostatic potential maps of analogs with pyrazine ring modifications, they identified a pharmacophore[13,14,16] for the formation of a stable blocking complex with the channel. An important steric feature of that pharmacophore is the distance between the proton donors of the guanidinium group and the minimum in the electrostatic potential off the chlorine at position 6 of the pyrazine ring. If analogs 18 and 19 are actually longer than amiloride, as indicated by their elongated side chains, then it is not clear

Table 1. Structure–activity relationships for selected amiloride analogs[a]

Analog number	R	pK_a	k_{on} (s^{-1}μM^{-1})	k_{off} (s^{-1})
1		8.67	13.17 ± 0.25	3.93 ± 0.19
18		4.50	1.22 ± 0.07	20.67 ± 3.72
19		9.00	2.16 ± 0.11	3.41 ± 0.55

[a]From Ref. 9.

how these molecules could fit the amiloride pharmacophore. Yet analog **19** actually forms a slightly more stable blocking complex than does amiloride with the sodium channel. Quantum mechanical conformational analysis of **18** and **19**,[16,17] however, revealed that **18** and **19** are nonplanar, with **19** being significantly less planar than **18**. Superposition of **18** and **19** onto amiloride, by fitting the chlorine atom and chelating hydrogens of the analogs to those of amiloride, seems to indicate that **18** and **19** can indeed fit the spatial requirements of the amiloride pharmacophore. Stereolithography was used to build plastic models of amiloride, **18**, and **19** in their global energy minimum conformers in order to investigate this relationship in more detail. In addition, a model of the "complementary surface" of amiloride, that is, an "impression" of the molecule in a solid block, was built to serve as a first approximation of the steric constraints that might be present in the sodium channel-binding site. The fit of the models of **18** and **19** into this model of the three-dimensional steric constraints of the pharmacophore was then examined.
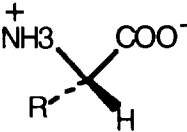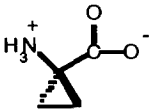
Structure–activity relationships of amino acid analogs

Small analogs of L-alanine, such as glycine, L-serine, β-chloro-L-alanine, and 1-amino-1-cyclopropane carboxylic acid, are excellent binders at the L-alanine taste receptor in the channel catfish, as illustrated by the low IC_{50} (50% inhibitory concentration) values in Table 2.[18] Alteration of the four groups attached to the α carbon allows for characterization of the steric and electrostatic properties that define a good binder at the taste receptor. In particular, for the active, zwitterionic forms of the analogs, analysis of the molecular shape restrictions imparted to the analogs by the other two substituents allows for characterization of the steric requirements for binding at the receptor, as well as some indication of the complementary steric nature of the receptor-binding pocket. Venanzi and co-workers[19] have developed a model of the steric and electrostatic features of the L-alanine-binding site of the catfish taste receptor. In addition, analysis of three-dimensional fixed models of the analogs in their global minimum energy conformations calculated in a dielectric approximating the receptor environment can assist in clarifying the picture of the dimensions and volume of the active site. For that reason, stereolithography models of the amino acids L-glycine, L-alanine, and L-serine, and the analogs β-chloro-L-alanine and 1-amino-1-cyclopropane carboxylic acid, were constructed from such calculated data.

Cyclodextrin catalysis

The cyclodextrins are known to accelerate the rate of acylation of a number of different substrates. Experimental observations show that cyclodextrins react with phenolic esters via an alkoxide ion derived from the secondary hydroxyl groups with the formation of a covalent intermediate and a subsequent release of corresponding phenols.[20-22] However, it is not clear whether the reaction occurs at the 2'- or 3'-hydroxyl group. A bound substrate has been observed to donate a nonequilibrating tosyl group to the 2'-hydroxyl.[23] On the other hand, direct tosylation of the 3'-hydroxyl has also been noted.[24] To provide further insight into the reactivity of cyclodextrins, Venanzi et al.[15] and Luzhkov and Venanzi[25] have used the semiempirical AM1 method[26] and the Langevin dipole solvent model[27-30] to study the reaction path of ester hydrolysis by hydroxide ion and by the alkoxide ions of β-cyclodextrin in gas phase and in polar environment. The purpose of the study was twofold: (1) To determine the role of the microenvironment provided by the macrocyclic cavity during the hydrolysis of acetate phenol, and (2) to determine if there is a difference in the reactivity of the secondary 2'- and 3'- hydroxyl oxygens of β-cyclodextrin. One of the results of the study was that acylation at the 3'-hydroxyl position is favored over the 2'-position by about 15 kcal/mol, owing to less structural reorganization of the macrocycle during hydrolysis at the 3' site. This is a situation in which a solid model of the cal-

Table 2. Structure–activity relationships for selected amino acid analogs[a]

Name	R	IC_{50} (M)	Neural response (%)
L-Alanine	$-CH_3$	3.5	100
β-Chloro-L-alanine	$-CH_2Cl$	2.5	88.6 ± 13.7
L-Serine	$-CH_2OH$	2	58.6 ± 15.6
Glycine	-H	3	62.3 ± 9.4
1-Amino-cyclopropane-1-carboxylic acid		3.7	78.3 ± 9.3

[a]From Ref. 18.

culated transition state[25] would be useful in interpreting the data. For that reason, stereolithography was used to build models of the neutron diffraction structure of β-cyclodextrin, consisting of 147 atoms, as well as a model of the transition state at the 2'-position. A model of the transition state at the 3'-position will be made in the future.

METHODS

Atomic coordinates

The low-energy conformations of the amino acids,[31] amiloride,[11] the two amiloride analogs,[17] and the transition state(s) of phenyl acetate cleavage by β-cyclodextrin[15,25] were determined by molecular orbital calculations, which are described in detail elsewhere. The global minimum energy coordinates of amiloride and the amiloride analogs were determined by conformational analysis, using the 6-31G* basis set. The global minimum energy coordinates of the amino acids and amino acid analogs were determined by the self-consistent reaction field (SCRF) method[32-36] in as described in Gaussian 92[37] using the 6-31G* basis set. Following Wong and co-workers,[35] the SCRF molecular radius was determined from the electronic density. The dielectric of 20.7 (acetone) was chosen to simulate the receptor environment. The transition state for β-cyclodextrin cleavage of phenyl acetate was determined using the AM1 method in the MOPAC-93 program.[38] The atomic coordinates of the neutron diffraction structure[39] of β-cyclodextrin undecahydrate were obtained from the Cambridge Structural Database.[40] All the water molecules were removed from the structure.

The structural information used to create the models was in the form of Cartesian coordinates of the atomic centers in ångstroms. Standard van der Waals radii were used for the atoms of all the models: H (1.2 Å), N (1.5 Å), O (1.4 Å), Cl (1.8 Å), and aliphatic C (2.0 Å), aromatic and carbonyl C (1.85 Å).[41] For the amino acid models, a van der Waals radius of 2.0 Å was used for all the carbon atoms.

The stereolithography process

The stereolithography apparatus (SLA) used was the model SLA-250 (shown in Figure 1) manufactured by 3D Systems (Valencia, CA). This apparatus consists of a cubic container (approximately 25.4 cm on a side) that holds the liquid resin. The resin used for these models was an acrylate ester blend consisting of aliphatic urethane acrylates, dimethylacrylate ester, and diacrylate ester (MSDS code number DL 1288). Within the cubic container of the SLA is a computer-controlled table that moves vertically. At the beginning of the building process, the table is elevated within the container holding the resin to a level that allows a specified thickness of resin to lie above the surface of the table. The computer-controlled laser then traces out, in the top layer of liquid resin, the shape of the lower slice of the object being built. This is a curing process that converts the liquid into a solid plastic material in the exact shape of the first slice of the object. The table with the first slice now atop its surface moves downward by a specified increment until another thin layer of liquid resin lies above the surface of the first slice. The laser then traces out the shape of the next slice,
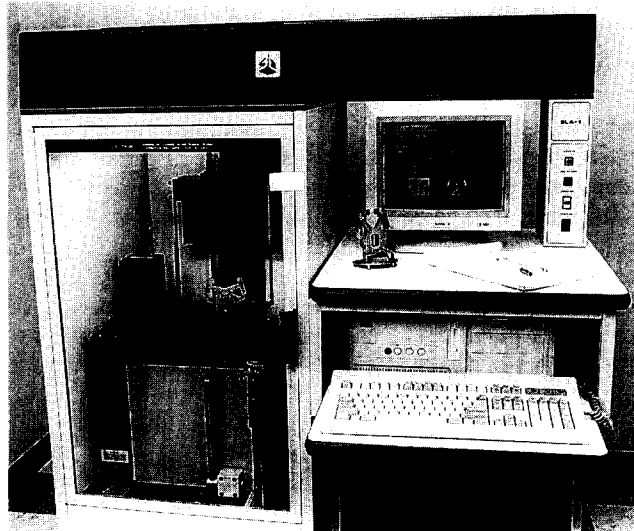

Figure 1. Stereolithography apparatus. (Photo credit: Bill Wittkop.)

again curing the liquid into a solid plastic and simultaneously bonding this second slice to the first. These operations are repeated until the entire object is built, slice by slice. On completion of the building process the table is again elevated to raise the model above the liquid. The model is removed, washed with isopropyl alcohol, and placed in an ultraviolet oven to complete the curing.

Creating the molecular model in the CAD program

The first step in the model-building process is to create a molecular model image in the CAD program. Several CAD programs can translate images into a format that can be read by the stereolithography apparatus. The program used here was I-DEAS,[42] version 6, installed on a Sun Sparcstation 10, model 41 (one processor, 96 MB RAM). A short program was written within I-DEAS to allow automatic input of the structural data from a text file. This input data consists of five parameters for each atom: the atomic symbol, the van der Waals radius, and the x, y, and z coordinates in ångstroms.

The coordinates of the first atom were input and a sphere of appropriate radius was drawn, creating the initial structure. The coordinates for the next atom, bonded to the ex-

Table 3. Stereolithography parameters

Parameter	Model	Support
Slice output scale	1.00	1.00
Resolution	5 000	5 000
Layer thickness[a]	0.013	0.025
X-Hatch spacing[a]	0.025	0.51
Y-Hatch spacing[a]	0.0	0.0
60/120° hatch spacing[a]	0.025	0.51

[a]Values in centimeters.

isting structure, were input and a second sphere drawn. At this point the CAD program recognizes the two spheres as individual objects despite the fact that they overlap in space. Here the Join command was invoked to merge the two spheres so that the program could recognize the overlapping spheres as a single object. This procedure was repeated for the remaining atoms in the molecule.

Rather than using completely smooth spheres to represent atoms, as is done in a molecular graphics program, the atom surfaces were varied by constructing them from facets. These facets are planar and yield a structure, which is essentially a polyhedron, as an approximation of a sphere. The number of facets along both the latitude and longitude of the sphere can be specified. The number of facets varied with the atom types for tactile and visual differentiation. The number of facets used for each atom type for all the models described here are as follows: H (8×8), C (8×8), O (12×12), N (16×16), Cl (20×20). The same number of facets were used for hydrogen and carbon atoms because these two atom types could still be readily distinguished by their size difference. As the number of facets increases, the surface approaches that of a smooth sphere. However, the file size also increases, requiring more time for subsequent processing and building.

Most models were constructed of solid spheres. However, models of 1-amino-1-cyclopropane carboxylic acid were also constructed with interior cavities in order to conserve material and reduce fabrication time. One model of 1-amino-1-cyclopropane carboxylic acid contained spherical cavities resulting in a wall thickness of 0.25 cm, whereas another model contained cubic cavities. A modified version of the input program was used to construct these two models, using spheres of smaller radii than the atomic radii, or cubes with edges equal in length to the radius of the given atom. These were then superimposed on the solid molecular model and their volumes cut (Cut command) from the molecule, leaving a continuous cavity within each molecular model. For these models, small holes had to be designed into the bottom of each model to allow the liquid resin to drain after completion of the building process. Because both internal and external surfaces had to be defined for these models, the resulting file sizes were larger than those for the solid model. The file sizes were as follows: solid model, 469,713 KB; model with cubic cavities, 602,409 KB; model with spherical cavities 1,055,205 KB.

The input dimensions were converted from ångstroms (1 Å = 0.64 cm) for the amiloride analogs, which resulted in carbon atoms of approximately 1.27-cm radius. The amino acids were made on a slightly larger scale (1 Å = 0.76 cm) while the β-cyclodextrin neutron diffraction and transition state models were built on a still larger scale (1 Å = 0.89 cm). To test the ability of the stereolithography technique to make small-scale, accurate models of macromolecules, the neutron diffraction structure was also built on a very small scale (1 Å = 0.19 cm). The input program also assigned appropriate colors to each atom for better visualization on screen. Each model was also moved into positive space within the CAD program so that the values of all coordinates are positive, as required for the succeeding steps.

Next, the Triangulate command in I-DEAS was invoked, which defines the points on the surface of the model in terms of triangular facets. Following this an STL file was generated that contains all the information necessary for stereolithography processing.

Creating the complementary shape of the amiloride molecule

Because amiloride has the most desirable pharmacological properties of the three molecules considered and has been shown to be planar in its lowest energy conformation in both gas phase[11] and solvent,[12] the complementary surface built to model the steric requirements of the pharmacophore was based on this structure. The complementary surface was defined simply as the impression that the amiloride model would make in a solid object.

The graphics image of the amiloride molecule used to create the impression was first enlarged by a factor of 1.1 relative to the size of the amiloride model actually built, so that the final model would fit easily into the impression. The planar molecule was then oriented horizontally and a solid rectangular block created. The top surface of the block was coplanar with the symmetry plane of the molecule. The dimensions of the block were made large enough to contain the impression of the molecule. Next, the Cut command in I-DEAS was invoked to remove from the rectangular block the space occupied by the molecule. This yielded a rectangular block with the impression of the amiloride molecule carved into one surface. A second complementary site was produced in a similar manner by creating a rectangular block that had its bottom surface coplanar with the symmetry plane of the molecule. This yielded a block with a complementary site that is a mirror image of the first. STL files were then created for these blocks as described above.

Construction of temporary support structures

Because of the layer-by-layer nature of the building process, it may not always be possible to orient the model in such a way that each slice consists of one continuous surface. This could lead to a situation in which a detached fragment of a slice is cured without having a solid structure below it. For example, spheres representing the atoms of some functional group may protrude at a downward angle from the side of the main structure. In this case one or more spheres would be lower than the point of attachment to the main structure and a horizontal slice at that level would consist of several disconnected parts. In addition, many models will have several points of contact with the elevator table of the SLA, resulting in the first few slices being disconnected. This problem is readily corrected by using a CAD program to design support structures that are removed after the model is built. The Bridgeworks[43] program was used to design these supports for the 1-amino-1-cyclopropane carboxylic acid and β-cyclodextrin models. The necessary supports for the other models were designed in I-DEAS and consisted simply of vertical cylinders attached to the bottoms of the spheres representing the atoms and extending to the base of the model. Separate STL files were then generated for the support structures for each model and were merged with the model files in a later step.

Preparation of files for stereolithography

Once the STL files for the models and supports have been generated, they must be further processed by the SLA. The first step involves processing by the Slice program[44] of the SLA Slice computer. This translates the data in the STL file into a format that represents the object as a series of horizontal slices which are the actual entities fabricated. At this point several parameters (see Table 3) are set that determine the resolution of the finished model and the rate of fabrication. The slice output scale is a factor determining the actual size of the final model relative to the dimensions specified in the CAD program. Resolution can be a value from 2 500 to 10 000, producing finer resolution as the value increases. Layer thickness is the actual thickness of each layer produced. A larger value for this parameter will produce a coarser surface, although the model will be fabricated more rapidly. A smaller value will produce a smoother surface but would require considerably more time to build. A larger value is used for the support structures because they are subsequently discarded.

At this point several Hatch Fill parameters are also set. Larger values for these parameters result in less resin being exposed to the laser light, resulting in weaker structures. Support structures usually have these parameters set to higher values to conserve resin and minimize fabrication time, and so that the resulting supports will be less substantial than the model and readily removed. After the slicing procedure an SLI file is generated for each object and its supports.

The next step is to invoke the Merge command in the SLA. This combines the SLI files for each object with the files created for its support structure into a series of files that will direct the building process. Files for several objects can also be merged at this point so that they can be built simultaneously. This completes the file processing prior to building of the models.

RESULTS

The plastic models produced by this method are shown in Figures 2–4. The models clearly represent the images described by the molecular orbital calculations and the neutron diffraction data. All atom types are readily identifiable.

The time required for the SLA to build the four amino acids and the 1-amino-1-cyclopropane carboxylic acid simultaneously was approximately 8 h. The building of three amiloride structures simultaneously required 12 h. The β-cyclodextrin model required 25 h to build and the β-cyclodextrin phenylacetate transition state model required 31 h. The curing process is usually completed with an additional 1–2 h in the ultraviolet (UV) curing oven. The temporary supports had been removed before placing the models in the oven. The Bridgeworks program optimized the support structures so that fewer and smaller temporary supports were built, reducing fabrication time and material consumption. This also resulted in a smoother surface after the supports were removed.

All models are sturdy and can withstand normal handling. Several of the smaller models, including one with the internal cavities, have been dropped onto a hard floor with-
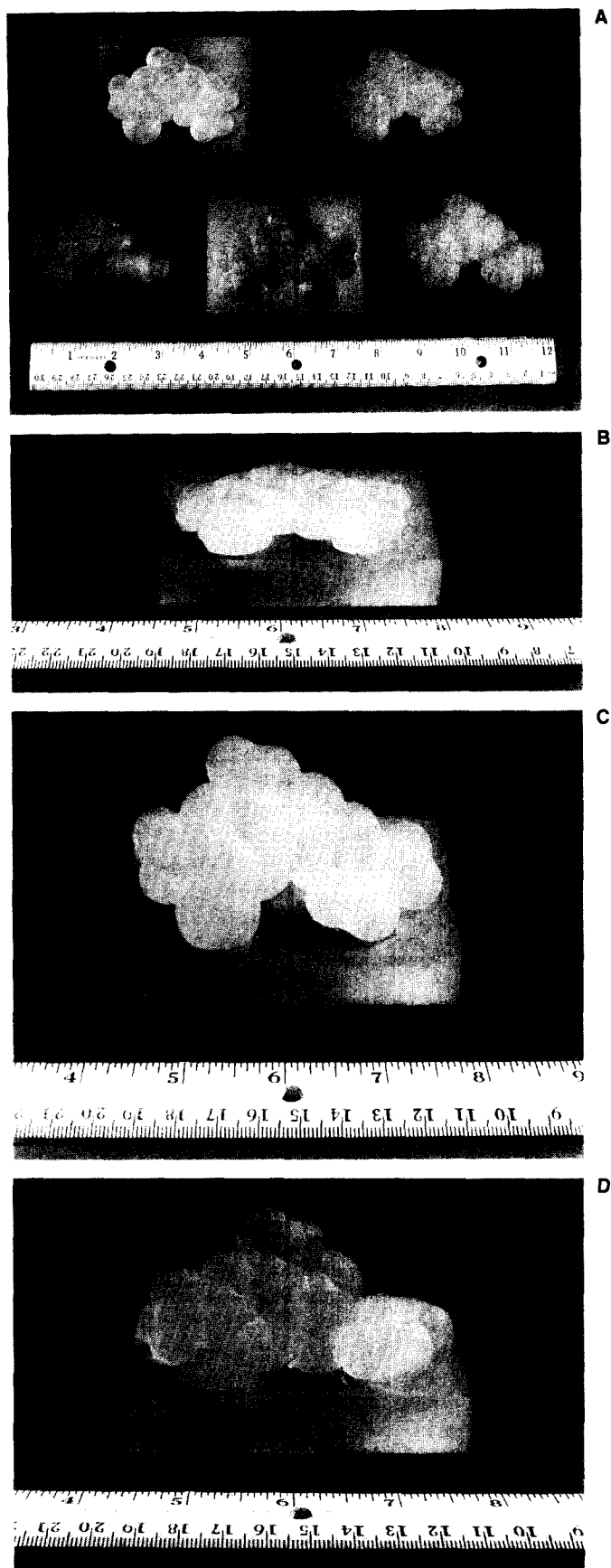
Figure 2. Solid models of amiloride analogs (approximately 7.5 × 6.25 cm in size) and amiloride complementary site. (A) Top row, from left: amiloride in complementary site; amiloride. Bottom row, from left: analog 19; mirror image of complementary site; analog 18. (B) Solid model of amiloride in complementary site. (C) Solid model of 18 in complementary site. (D) Solid model of 19 in complementary site. (Photo credit: Bill Wittkop.)
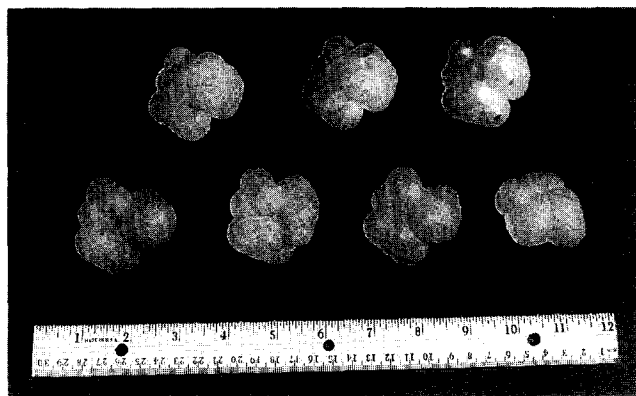
Figure 3. Models of amino acids and analogs (approximately 5 cm across), all oriented with the amino group on the top left side and the carboxylate group on the bottom left side. Top row from left: 1-amino-1-cyclopropane carboxylic acid (solid model, hollow model, and another hollow model). Bottom row, from left (solid models): β-chloro-L-alanine, L-alanine, L-serine, glycine. (Photo credit: Bill Wittkop.)

out damage. The three models of 1-amino-1-cyclopropane carboxylic acid were weighed, yielding the following values: solid, 49 g; cubic cavities, 32 g; spherical cavities, 20 g. This indicates that the fabrication of hollow models results in a significant reduction in the amount of resin consumed and, because their structural strength was still substantial, this can represent a more efficient method of fabrication.

Amiloride models

Figure 2A shows the amiloride models and the complementary sites. Figure 2B shows a close-up view of amiloride in the complementary site, which emphasizes the planarity of the molecule. This is in contrast to the orientations of analogs 18 and 19 in the site described below. The spatial relationships of the models of the nonplanar amiloride analogs 18 and 19 with the model of the "impression" of the planar amiloride molecule were examined, with particular attention given to the relative positions of the components of the pharmacophore. Placing the chlorine atom of analog 18 into the impression made by the chlorine atom of amiloride and manipulating the models shows that the guanidinium hydrogen atoms are not far from the analogous sites that would be occupied by those of amiloride. This can be seen from Figure 2C, which shows that the pyrazine ring of analog 18 cannot be coplanar with the impression of the amiloride pyrazine ring in the complementary site if the steric requirements of the amiloride pharmacophore are to be met. Figure 2C also shows that it is somewhat difficult for the chlorine atom and the guanidinium hydrogens to coincide simultaneously with their complementary locations in the amiloride site. Similar manipulation of the model of analog 19, however, shows a closer match of the guanidinium hydrogens and chlorine of 19 to the locations on the complementary site that would be occupied by those of amiloride. Figure 2D shows that, in this case, the pyrazine

ring of 19 is nearly perpendicular to the orientation it assumes in amiloride, while the chlorine and guanidinium hydrogens approach the amiloride pharmacophore closely. This is consistent with the experimental kinetic data in Table 1, which show that 19 is a slightly better sodium channel blocker than 1.

Because the sodium channel blocking process involves at least two steps, the first involving the guanidinium side chain approach to the binding site and the second step the binding of the chlorine atom to a site on the channel, these models demonstrate that the steric requirements can be somewhat satisfied by analogs 18 and 19 in these global energy minimum conformations. Applying this procedure to the same molecular models with the mirror image of the amiloride impression does not yield a close fit for either analog 18 or 19, suggesting further steric requirements for the channel-binding site.

Amino acid models

Figure 3 shows that the shapes of the molecules that are the best binders at the L-alanine receptor are similar to each other. The relative placement of the carboxylate (bottom left side) and amino (top left side) moieties is almost identical in each case, the one exception being the slight tilt of the carboxylate group in L-serine. The β carbon and its substituent group (center) are directed toward the viewer. It can be seen that it is generally located in the same region of space for all the analogs. The volume of the analog and the steric requirements for binding are nearly identical for each of these analogs. This idea was first suggested by Bryant et al.,[18] but is clearly exemplified by this set of models. Work
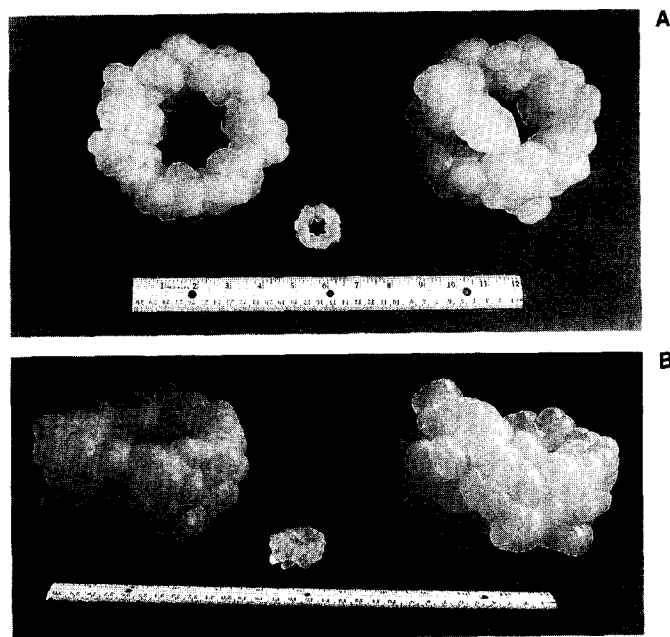

Figure 4. Solid models of cyclodextrins. From left: Neutron diffraction structure (15 cm in diameter, 7.5 cm high); scaled-down neutron diffraction structure (3.7 cm in diameter, 1.8 cm high); transition state structure for phenyl acetate cleavage by 2'-hydroxyl oxygen. (A) Top view. (B) Side view. (Photo credit: Bill Wittkop.)

is ongoing to produce a steric model of the tastant receptor site based on these structures.

Cyclodextrin models

The models of β-cyclodextrin and its transition state complex with phenylacetate at the 2'-hydroxyl oxygen were fabricated on a larger scale in order to allow easy examination of the cavity. They are shown in Figure 4. The top and side views of the cavities illustrate that the model based on the neutron diffraction data clearly shows how the seven glucose units combine to form the macrocycle. The orientations of the hydroxyl groups along both openings of the cavity are readily distinguished. The model of the transition state complex at the 2'-hydroxyl shows the orientation of the phenyl acetate within the cavity, clearly depicting the point of contact of the phenyl ring with the macrocycle and the degree to which the substrate extends above the plane of the rim of the cavity. The small-scale version of the neutron diffraction structure (center) contains, remarkably, all the features of the large model.

DISCUSSION

The models used here are particularly suited to investigation of steric questions because they were designed using van der Waals radii. In fact, a model of just the steric requirements of the pharmacophore could be built. However, the method is not limited to building this type of model. Different atomic radii appropriate for other investigations can be specified. Work is currently being done on procedures for building models that represent the spatial distribution of other physical properties. Specifically, we are attempting to develop meaningful models representing the electrostatic potential and the electron density. The powerful features of the CAD programs allow considerable manipulation of images. Another area of investigation is the superposition of the images of two or more molecules and the fabrication of a model of the space they occupy in common. The CAD programs also allow rotation about designated axes and can create an image of the space swept by an object during the rotation. Selected parts of a molecule could be rotated through specific torsional angles about molecular bonds and the space occupied by the atoms as they move could be made into a solid model. In this way the steric properties exhibited by a molecule over a range of conformations can be examined. The torsional angles can be chosen on the basis of specific energy constraints, allowing dynamic processes to be modeled.

As shown above, this method can also be applied to the building of accurate models of proposed transition states, which may not be possible using other modeling techniques. Virtually any proposed geometry can be depicted in these models.

Biological macromolecules can be modeled despite the size limitations of this particular instrument. The small-scale model of the neutron diffraction structure of cyclodextrin illustrates that structural information can be accurately portrayed in a very small model. Or, if a large model is preferred, an image created in the CAD program can be cut into several smaller parts that can be built separately and

combined to form the entire structure. Tabs and holes can be added to ensure that the parts are assembled accurately. The docking of small molecules with proteins or nucleic acids can be examined with such models. A model of the macromolecule can be built according to appropriate structural data and used to examine the conformational relationships with models of many ligand molecules. In certain cases it may be unnecessary to construct the model of an entire macromolecule. This method has the ability to allow the selection of the appropriate region of the molecule of interest and build only that portion. The SLA-500 model (with tank dimensions 50.8 × 50.8 × 60.96 cm) is also available for constructing larger models in a single step.

Some CAD programs allow images to be defined by mathematical functions that could then be translated into plastic models. Models can then be constructed of maps of various physical properties that have specific spatial distributions. We are currently developing ways to represent three-dimensional maps of molecular electrostatic potentials, using this method.

The plastic models produced are uncolored and translucent but can be painted to improve the visibility of specific atoms and surface features. We are investigating the use of coded surface features to aid in both visual and tactile perception.

Such models can also be useful as teaching aids on all levels. Complex molecular structures, molecular orbitals, crystal lattices, and cell organelles are only a few of the systems with important spatial relationships that could be modeled and provide students with additional insights. Other manufacturing techniques[45] might then be applied to mass produce specific models for distribution to educational institutions.

REFERENCES

1 Emery, J. Stereolithography Models and Prototypes. *US DOE Technical Report KCP-613-5429*. National Technical Information Service, Springfield, Virginia 1994

2 Burns, M. *Automated Fabrication*. Prentice Hall, Englewood Cliffs, New Jersey 1993

3 Hull, C. Stereolithography: Plastic prototypes from CAD without tooling. *Mod. Cast.* 1988, **78**, 38

4 Heinzmann, H. Stereolithography—the fast way from 3D CAD model to prototypes. *Kautsch. Gummi, Kunstst.* 1993, **46**, 19–21

5 Schmitt, H., Geiger, M., and Steger, W. Stereolithography in original model production. *Konstr. Giessen* 1992, **17**, 13–19

6 Bisschop, L. and Jagt, J.C. Stereolithography: A com-

bination of CAD, laser technology, and UV-polymerization. *Kustst. Rubber* 1992, 11–18

7 Neckers, D.C. Stereolithography: An introduction. *CHEMTECH* 1990, **20**, 615–619

8 Skawinski, W.J., Busanic, T.J., Ofsievich, A.D., Luzhkov, V.B., Venanzi, T.J., and Venanzi, C.A. The use of laser stereolithography to produce three-dimensional tactile models for blind and visually impaired scientists and students. *Inf. Technol. Disabilities* 1994, 1(No. 4, Article 6), 1994

9 Li, J.H.-Y., Cragoe, E.J., Jr., and Lindemann, B. Structure-activity relationship of amiloride analogs as blockers of epithelial Na channels. II. Side-chain modifications. *J. Membr. Biol.* 1987, **95**, 171–185

10 Li, J.H.-Y. Cragoe, E.J., Jr., and Lindemann, B. Structure-activity relationship of amiloride analogs as blockers of epithelial sodium channels. I. Pyrazine-ring modifications. *J. Membr Biol.* 1985, **83**, 45–56

11 Venanzi, C.A., Plant, C., and Venanzi, T.J. A molecular orbital study of amiloride. *J. Comput. Chem.* 1991, **12**, 850–861

12 Buono, R.A., Venanzi, T.J., Zauhar, R.J., Luzhkov, V.B., and Venanzi, C.A. Molecular dynamics and static solvation studies of amiloride. *J. Am. Chem. Soc.* 1994, **116**, 1502–1513

13 Venanzi, C.A., Plant, C., and Venanzi, T.J. Molecular recognition of amiloride analogs: A molecular electrostatic potential analysis. 1. Pyrazine ring modifications. *J. Med. Chem.* 1992, **35**, 1643–1649

14 Venanzi, C.A. and Venanzi, T.J. Molecular modeling studies of amiloride analogs. In *Mechanisms of Taste Transduction* (Simon, S.A. and Roper, S.D., Eds.). CRC Press, Boca Raton, Florida, 1993, pp. 428–462

15 Venanzi, C.A., Buono, R.A., Luzhkov, V.B., Zauhar, R.J., and Venanzi, T.J. Case studies in solvation of bioactive molecules: Amiloride, a sodium channel blocker; β-cyclodextrin, an enzyme mimic. In *Structure and Reactivity in Aqueous Solution: Characterization of Chemical and Biological Systems* (Cramer, C.J. and Truhlar, D.G., Eds.). ACS Symposium Series **568**, American Chemical Society, Washington, D.C., 1994, pp. 260–280

16 Venanzi, C.A., Buono, R.A., Skawinski, W.J., Busanic, T.J., Venanzi, T.J., Zauhar, R.J., and Luzhkov, V.B. From maps to models: A concerted computational approach to analysis of the structure-activity relationships of amiloride analogues. In *Computer-Aided Molecular Design: Applications in Agrochemicals, Materials, and Pharmaceuticals* (Reynolds, C.J., Holloway, M.K., and Cox, H.K., Eds.). ACS Symposium Series **589**, American Chemical Society, Washington, D.C., 1995, pp. 51–63

17 Skawinski, W.J. and Venanzi, C.A. 1995 (in preparation)

18 Bryant, B.P., Leftheris, K., Quinn, J.V., and Brand, J.G. Molecular structural requirements for binding and activation of L-alanine taste receptors. *Amino Acids* 1993, **4**, 73–88

19 Venanzi, T.J., Bryant, B.P., and Venanzi, C.A. Modeling of the L-alanine receptor in the channel catfish. 1995 (in preparation)

20 Bender, M.L. and Komiyama, M. *Cyclodextrin Chemistry*. Springer-Verlag, Berlin, 1978

21 Bender, M.L., Bergeron, R.J., and Komiyama, M. *The Bioorganic Chemistry of Enzymatic Catalysis*. John Wiley & Sons, New York, 1984

22 Breslow, R. Adjusting the lock and adjusting the key in cyclodextrin chemistry: An introduction. *Adv. Chem. Ser.* 1980, **191**, 1–15

23 Ueno, A. and Breslow, R. Selective sulfonation of a secondary hydroxyl group of β-cyclodextrin. *Tetrahedron Lett.* 1982, **23**, 3451–3454

24 Fujita, K., Tahara, T., Imoto, T., and Koga, T. Regiospecific sulfonation onto C-3 hydroxyls of β-cyclodextrin. Preparation and enzyme-based assignment of 3A, 3C and 3A, 3D disulfonates. *J. Am. Chem. Soc.* 1986, **108**, 2030–2034

25 Luzhkov, V.B. and Venanzi, C.A. Computer modeling of phenyl acetate hydrolysis in water and in reaction with β-cyclodextrin: Molecular orbital calculations with the semiempirical AM1 method and the langevin dipole solvent model. *J. Phys. Chem.* 1995, **99**, 2312–2323

26 Dewar, M.J.S., Zoebisch, E.G., Healy, E.F., and Stewart, J.J.P. AM1: A new general purpose quantum mechanical molecular model. *J. Am. Chem. Soc.* 1985, **107**, 3902–3909

27 Warshel, A. *Computer Modeling of Chemical Reactions in Enzymes and Solutions*. John Wiley & Sons, New York, 1991

28 Warshel, A. and Russel, S. Calculations of electrostatic interactions in biological systems and in solutions. *Q. Rev. Biophys.* 1984, **17**, 283–422

29 Lee, F.S., Chu, Z.T., and Warshel, A. Microscopic and semimicroscopic calculations of electrostatic energies in proteins by the POLARIS and ENZYMIX programs. *J. Comput. Chem.* 1993, **14**, 161–185

30 Luzhkov, V. and Warshel, A. Microscopic models for quantum mechanical calculations of chemical processes in solutions: LD/AMPAC and SCASS/AMPAC calculations of solvation energies. *J. Comput. Chem.* 1992, **13**, 199–213

31 Venanzi, T.J. and Venanzi, C.A. 1995 (in preparation)

32 Wong, M.W. and Wiberg, K.B. Hartree-Fock second derivatives and electric field properties in a solvent reaction field: Theory and application. *J. Chem. Phys.* 1991, **95**, 8991–8998

33 Wong, M.W., Frisch, M.J., and Wiberg, K.B. Solvent effects. 1. The mediation of electrostatic effects by solvents. *J. Am. Chem. Soc.* 1991, **113**, 4776–4782

34 Wong, M.W., Wiberg, K.B., and Frisch, M.J. Solvent effects. 2. Medium effect on the structure, energy, charge density, and vibrational frequencies of sulfamic acid. *J. Am. Chem. Soc.* 1992, **114**, 523–529

35 Wong, M.W., Wiberg, K.B., and Frisch, M.J. Solvent effects. 3. Tautomeric equilibria of formamide and 2-pyridone in the gas phase and in solution. An ab initio SCRF study. *J. Am. Chem. Soc.* 1992, **114**, 1645–1652

36 Wiberg, K.B. and Wong, M.W. Solvent effects. 4. Effect of solvent on the E/Z energy difference for methyl formate and methyl acetate. *J. Am. Chem. Soc.* 1993, **115**, 1078–1084

37 Frisch, M.J., Trucks, G.W., Head-Gordon, M., Gill, P.M.W., Wong, M.W., Foresman, J.B., Johnson, B.G., Schlegel, H.B., Robb, M.A., Replogle, E.S.,

Gompers, R., Andres, J.L., Raghavachari, K., Binkley, J.S., Gonzalez, C., Martin, R.L., Fox, D.J., Defrees, D.J., Baker, J., Stewart, J.J.P., and Pople, J.A., *Gaussian 92, Release A*. Gaussian, Inc., Pittsburgh, Pennsylvania, 1992

38 Stewart, J.J.P. *MOPAC-93 Manual*. Fujitsu, Ltd., Tokyo, Japan, 1993

39 Betzel, C., Saenger, W., Hingerty, B.E., and Brown, G.M. Circular and flip-flop hydrogen bonding in β-cyclodextrin undecahydrate: A neutron diffraction study. *J. Am. Chem. Soc.* 1984, **106**, 7545–7557

40 Allen, F.H., Kennard, O,. and Taylor, R. Systematic analysis of structural data as a research technique in organic chemistry. *Acc. Chem. Res.* 1983, **16**, 146–153

41 Weast, R.C. (Ed.). *CRC Handbook of Chemistry and Physics*. CRC Press, Boca Raton, Florida, 1979–1980, p. D-194

42 *I-DEAS*. Available from SDRC, Inc., Milford, Ohio

43 *Bridgeworks*. Available from Solid Concepts, Valencia, California

44 *Slice*. Available from 3D Systems, Valencia, California

45 Imamura, M., Meng, Y., and Nakagawa, T. Application of laser stereolithography to castings. *Seisan Kenkyu* 1993, **45**, 385–392